

SELF-ASSEMBLY OF CARBON NANOTUBES

D. TOMÁNEK

*Department of Physics and Astronomy, Michigan State University, East Lansing,
Michigan, 48824-1116, USA*

Carbon nanotubes, consisting of graphitic cylinders, have been synthesized in bulk quantities. This contribution summarizes our present knowledge of the microscopic mechanisms leading to the self-assembly of single-wall or multi-wall tubes. Numerical calculations, supported by experimental evidence, suggest these close relatives of fullerenes to be extremely stable with respect to mechanical stresses or applied electric fields.

Until relatively recently, the only stable forms of pure elemental carbon have been believed to be graphite and diamond. This conventional wisdom has been revolutionized by the discovery of the C_{60} "buckyball"¹ and other related fullerenes², in particular carbon nanotubes.^{3,4}

Single-wall carbon nanotubes, consisting of a graphene sheet seamlessly wrapped to a cylinder, have been produced in the outflow of a carbon⁵⁻⁹ and in even higher yield by laser vaporization¹⁰⁻¹³ of graphite enriched by a transition metal catalyst. Formation of multi-wall tubes, on the other hand, has been traditionally associated with external factors such as strong electric fields^{3,4,14-17} or surfaces at low temperature.^{18,19} More recently, tubes have been observed to form by laser vaporizing pure graphite, in the absence of any of these external factors.^{11,12}

While a large variety of fullerene-based structures has been successfully synthesized, experimental data provide little insight into the microscopic mechanisms leading to self-assembly (or destruction) of these systems. In particular, one would like to learn about the optimum conditions which would lead to the preferential formation of single- or multi-wall nanotubes rather than single- or multi-wall fullerenes, bulk graphite, or diamond. Equally interesting as the microscopic self-assembly mechanism of nanotubes is a detailed knowledge of their decay mechanism in high electric fields, which is important for their application as nanostructured field electron emitters.

In the following, after presenting a brief summary of theoretical methods, I will discuss the morphology and the self-assembly mechanisms of single- and multi-wall nanotubes. Carbon nanotubes, same as fullerenes, will be shown to be mechanically very resilient and extremely stable in applied electric fields.

Molecular dynamics formalism

Microscopic processes associated with the formation and disintegration of nanostructures such as carbon nanotubes occur on the short length scale of 10^{-9} m and equally short time scale of 10^{-13} s, beyond the scope of direct experimental observation. The only way to obtain information about the trajectories of individual atoms is to perform a molecular dynamics simulation. These simulations provide

information not only about the time evolution of cluster geometries, but also about the thermodynamic behavior of these systems.

The Lagrangian describing the atomic aggregate as a microcanonical ensemble is given by the classical expression $\mathcal{L} = \sum_{i=1}^N \frac{1}{2} m_i \dot{q}_i^2 - V(\{\vec{q}\})$, where q_i and m_i are the coordinates and the masses of the individual particles, respectively, and V the potential energy of the system. A canonical ensemble, where the temperature rather than the total energy is conserved, can be described by the Nosé-Hoover Lagrangian,²⁰ where an additional, virtual degree of freedom is used to equilibrate the system with an external “heat bath” of constant temperature. Individual atomic trajectories are obtained by integrating the Euler-Lagrange equations of motion. The crucial quantity is the potential energy $V(\{\mathbf{q}_i\})$ of the system, which is a non-trivial many-body functional.

For a given structure, most insight can be obtained from an *ab initio* calculation, typically based on the density functional formalism. To address the dynamical evolution of a system for long times, parametrized total energy functionals have been shown to yield reliable results within useful time scales on massively parallel supercomputers, such as the Cray T3E.

Density functional formalism

Perhaps the most powerful *ab initio* technique used in total energy calculations of complex systems - such as fullerenes or nanotubes - is the Density Functional Theory (DFT).²¹ It is based on the Kohn-Sham theorem stating that in the ground state, the total electronic energy of a given system is a unique functional of the total charge density $\rho = \rho(\vec{r})$ that can be obtained in a variational manner. Practically, the nontrivial exchange-correlation part of this functional is often parametrized either as a local function of $\rho = \rho(\vec{r})$ in the Local Density Approximation (LDA),^{21,22} or as a nonlocal functional in the Generalized Gradient Approximation (GGA).²³ Tube ends, where the most interesting phenomena occur, can be efficiently described by cluster fragments. Edge effects can be controlled by saturating the dangling bonds with hydrogen.

In general, *ab initio* DFT calculations are computationally very intensive. For this reason, many parametrized techniques compete successfully with this formalism.

Parametrized Linear Combination of Atomic Orbitals (LCAO) formalism

In recent years, it has been shown that the parametrized Linear Combination of Atomic Orbitals (LCAO) formalism provides a computationally efficient and reliable approach to determine the electronic spectrum and the total energy of large systems. This one-electron technique provides us with a physically sensible way to extrapolate *ab initio* results to systems with low symmetry. The general expression for the total energy of a carbon aggregate,²⁴ which uses the total electronic density of states, provides the possibility to calculate also the binding energy of individual atoms, using the local density of states. The latter quantity can be efficiently evaluated within the recursion

technique.²⁵ This approach results in linear scaling of the computer resources with the number of particles [$O(N)$ technique], and a conceptually straightforward implementation on massively parallel computers. The computational efficiency of this approach is of great advantage when computing structural and electronic properties of very large carbon systems, and in molecular dynamics simulations.

I will summarize the usefulness of the above formalism when addressing the formation and disintegration of nanotubes. First, I will discuss the equilibrium structure and classification of nanotube systems. Next, I will address the formation mechanism of single- and multi-wall nanotubes. Finally, I will briefly summarize our knowledge of the high structural rigidity and stability of nanotubes in high electric fields.

Morphology of carbon nanotubes

Carbon nanotubes consist of graphene sheets wrapped to a cylinder. All atoms have the same distance from the tube axis, typically only few nanometers. Charge distribution and electronic structure are closely related to those of graphite (and fullerenes). The strong covalent graphitic bonds are responsible for the structural rigidity of nanotubes. Single-wall nanotubes can bundle up to a triangular crystalline lattice, as a cylindrical analogy to the C_{60} solid composed of identical (single-wall) C_{60} molecules. Nanotubes can also be found nested inside each other, as “matryoshka structures”, analogous to the multi-shell “bucky onions”. In both cases, the distance between adjacent walls is $\sim 3.4 \text{ \AA}$, maintained by weak inter-wall bonds (with both covalent and van der Waals contributions), similar to the weak inter-layer bonds in graphite.

(n, m) nanotubes can be characterized by the chiral vector $\mathbf{C}_h = n\mathbf{a}_1 + m\mathbf{a}_2$ on the honeycomb lattice of a flat graphene sheet,² where \mathbf{a}_1 and \mathbf{a}_2 denote the lattice vectors of graphite. The cylinders are formed by rolling up the graphene sheet so that sites defined by lattice vector \mathbf{R} fall on top of sites given by the lattice vector $\mathbf{R} + \mathbf{C}_h$. The chiral angle θ is given with respect to the $(\mathbf{a}_1 + \mathbf{a}_2)$ direction. One typically distinguishes achiral nanotubes with a “zig-zag” edge, $(n, 0)$, tubes with an “armchair” edge, (n, n) , and other, chiral nanotubes. Because of the sixfold symmetry of the honeycomb lattice, several different integer pairs (n, m) describe equivalent tubes. In analogy to fullerenes, nested (multi-wall) nanotubes can be characterized by $(n_1, m_1)@(n_2, m_2)@...$. Theoretical studies have shown that chirality has a profound effect on the electronic structure of isolated single-wall nanotubes.^{26,27}

Growth of single-wall nanotubes

Single-wall carbon nanotubes, with no amorphous overcoating, have been synthesized with a $\geq 70\%$ yield by laser vaporization of graphite with $\leq 1\%$ Co-Ni catalyst.¹⁰ The samples consist predominantly of identical (10,10) tubes, up to 0.1 mm long, that bundle up to form “ropes”. The ropes consist of an ordered triangular lattice of tubes, and are metallic, with a resistivity of $\rho < 10^{-4} \Omega\text{-cm}$ for single ropes at $T = 300 \text{ K}$.

From the theoretical point of view, there are several intriguing points awaiting an answer. Why does laser vaporization of metal-enriched graphite produce only single-wall tubes and not other fullerenes? Why is the tube diameter universal and independent of the catalyst? How do the nanotubes grow, and which is the role of the metal catalyst

in the growth process? The key to the answer is knowing the structure and energetics of the growing tube nucleus.

Based on *ab initio* and parametrized LCAO calculations, as well as continuum elasticity theory, we conclude that the 14 Å tube diameter is kinetically fixed in the early growth stage, when the tube contains only a few hundred atoms^{10,28} (Figure 1). The higher stability of the armchair edge (as compared to the zig-zag edge) favors (10,10) tubes. These tubes are capped at one end by half of the “magic” C₂₄₀ fullerene of icosahedral symmetry.

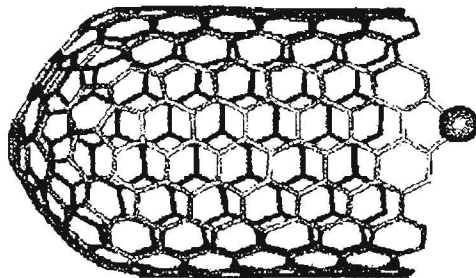


Figure 1 Growing (10,10) nanotube nucleus. The cap on one side is half the C₂₄₀ fullerene. The other end is kept open by a metal catalyst atom “scooting” around the edge.¹⁰

Our *ab initio* calculations suggest that the transition metal catalyst prefers to bind in atomic form to carbon. The most favorable adsorption sites on a (10,10) nanotube are at the exposed, growing edge. The Ni-tube bond strength (6.4 eV from LDA and 4.7 eV from GGA) is sufficient to prevent the catalyst from evaporating under synthesis conditions. A relatively small diffusion barrier of ≈1 eV gives the Ni atom a high mobility along the tube edge. Using a concerted exchange mechanism, adsorbed Ni atoms catalyze the continuing assembly of carbon hexagons from carbon feedstock, predominantly consisting of short chains diffusing along the nanotube wall. Presence of this mobile, atomic catalyst is essential to anneal pentagon defects that would otherwise lead to a premature dome closure of the nanotube.

Growth of multi-wall nanotubes

The intriguing discovery that nanotubes can be generated by laser vaporizing pure graphite,^{11,12} in the absence of any spatial anisotropy or other factors favoring oblong objects, raised several questions. First of all, one would like to know why the same experimental setup, with only small changes in laser power or focussing, can in one case produce tubes and in the other case spherical fullerenes. It is rather puzzling that the tubes are rather long, perfect, inert, and have mostly an even number of walls.

As for the self-assembly of single-wall nanotubes, the key to the answer is the atomic structure at the growing edge of the nanotube. Since all nanotubes grown by laser vaporization of graphite have multiple walls, we consider a double-wall nanotube as the simplest model system. The specific question is, whether carbon chains and atoms in the atmosphere prefer to adsorb independently at the reactive, exposed edges, or rather prefer to

bridge the gap between the adjacent walls by covalent bonds, establishing an effective "lip-lip interaction".¹¹

Our results,^{29,30} based on structural optimization using both *ab initio* and parametrized LCAO techniques, suggest that for specific adsorption geometries, a covalent "lip-lip interaction" can stabilize the tube end by up to ≤ 0.5 eV per added C atom at the "lip" with respect to the reference geometry containing added atoms at individual tube edges. The stabilizing "lip-lip" interaction via covalent bonds connecting adjacent tube edges has several important consequences, which also answer most of the puzzles mentioned above.

The necessary prerequisite for the growth of a long tube (rather than a spherical fullerene) is a mechanism which would inhibit early dome closure of the tube at the growing end, yielding a double-wall capsule. For a double-wall tube, dome closure due to the insertion of a pentagon defect at the inner wall could occur only at the cost of breaking the covalent "lip-lip" bonds. Hence, by inhibiting dome closure of only one of the two tubes, the growth is much less likely to terminate spontaneously. With nonzero probability, two pentagon defects will eventually form simultaneously at the growing edge of adjacent walls, initiating a closure as a double dome. Since this probability is rather low, carbon nanotubes tend to grow long.

Continued growth involves concerted rearrangement of the "lip-lip" bonds at the growing edge during carbon accretion. The exothermic nature of the process results from the binding energy gain associated with the incorporation of carbon atoms from the atmosphere, consisting predominantly of linear aggregates, in the graphitic lattice of the nanotube.

As saturation of dangling bonds at the growing edge of the nanotubes slows down their growth, defects have time to heal out. This may be an important reason why nanotubes are relatively defect-free. The absence of dangling bonds at the growing edge of a double-wall nanotube due to the presence of covalent "lip-lip" bonds seems to reduce drastically the reactivity of the nanotube with respect to oxygen. This finding is supported by the fact that single-wall tubes, containing unsaturated dangling bonds at the growing edge, are unstable in oxygen atmosphere.

Once a double-wall nanotube has formed, it can serve as a template for further fattening. This will proceed by accretion of graphitic overlayers, preferentially arranged as concentric cylinders. Due to the presence of dangling bonds at the exposed edge, a growing single-wall shell is unlikely to survive the etching effect of oxygen in the atmosphere. A double-wall outer shell, on the other hand, has the dangling bonds saturated at the edge, and consequently a much better chance of survival. This may be the reason for the relative abundance of multi-wall nanotubes with an even number of walls, observed in transmission electron microscopy images.^{3,5,31}

Rigidity of carbon nanotubes

Calculated vibrational spectra of capped (5,5) nanotubes of different lengths are very similar to the C_{60} spectrum.³² The lowest frequency vibration modes of nanotubes are bending modes, which contain information about the "beam rigidity" of these structures. We found a very high value $c_B = F/\Delta z = 2.1 \cdot 10^3$ dyn/cm for the "spring constant" associated with the bending of a C_{400} nanocapsule.³² Converting this quantity into a bulk elastic constant of a "nanotube material" yields values for the Young's modulus close to

$Y = 5 \text{ TPa}$.³² This high value has been confirmed by an experimental observation of an exceptionally high Young's modulus $Y = 4 \text{ TPa}$ of the nanotube material, deduced from transmission electron microscope observations of individual carbon nanotubes.³³

Disintegration of nanotubes

When exposed to a high electric field, individually mounted multi-wall nanotubes have been demonstrated to emit electron currents of up to several microamperes.³⁴ This immediately suggests their possible application as ultimate field electron emitters,^{34,35} possibly in flat panel displays.³⁶

Several puzzling phenomena were discovered when observing the field emission current of an isolated carbon nanotube,³⁴ which are related to the stability and disintegration of nanotubes in high electric fields. Whereas exposing the tube tip to a laser beam increased the current in low fields, the emission current in high fields was efficiently quenched by laser heating the tip, or by exposing the nanotube to residual gas. The emission current was observed to fluctuate in discrete steps, and a constant dim glow at the tip of the tube was observed, with occasional flare-ups in a much larger region of the whole tube, followed by the same dim glow at the tip.

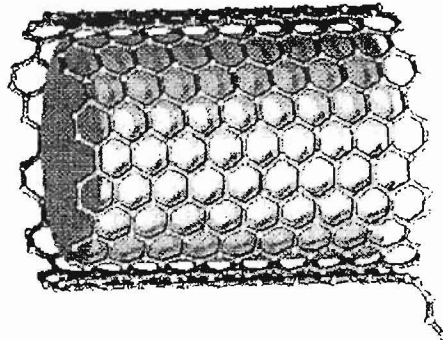


Figure 2 Unraveling of a chiral single-wall nanotube. Even at $T = 2000 \text{ K}$, in zero applied field, a stable monatomic carbon "wire" remains firmly attached to the tube.

The key to addressing these questions lies in the microscopic structure of the tube tip in high electric fields. In the following, I will summarize theoretical results of References 29, 37 supporting the conjecture of Reference 34 that the large emission currents observed originate from "atomically sharp" structures. Structures such as monatomic "carbon wires" dangling off the edge (as shown in Figure 2), it was argued, may be the ultimate field electron emitters.^{34,38,39}

A double-wall $(9,0)@(18,0)$ zig-zag nanotube with an open edge was used in the *ab initio* calculation used to address this problem theoretically.³⁷ The exposed tube edges were locally stabilized by a covalent "lip-lip" interaction discussed in the previous Section. This calculation showed that charge-neutral "zig-zag" nanotubes are extremely stable in high electric fields below 3 V/\AA . In higher fields, chiral tubes start

disintegrating, by preferentially unraveling carbon chains from the exposed edge, like a pullover sleeve. Unraveling monatomic carbon chains not only withstand fields up to 3 V/\AA ,⁴⁰ but also increase the field locally near their end, thus enhancing electron emission.

This unraveling process is facilitated when excess electrons, due to tube polarization, accumulate at the exposed tube end. These extra electrons populate antibonding orbitals and thus facilitate evaporation of ions from the exposed chain end at somewhat lower fields of $\approx 2 \text{ V/\AA}$. Our calculations show that the covalent "lip-lip" bonds connecting adjacent wall edges are strong enough to terminate the unraveling process at these high field values.

I have discussed successful application of both *ab initio* and parametrized techniques to quantitative calculations of the formation, stability, and fragmentation of carbon nanotubes.

Theoretical results indicate that the universal diameter of *single-wall tubes* results from optimizing the initial nucleus and reflects the energetics of graphite. Metal catalyst atoms efficiently anneal defects at the exposed edge, thus inhibiting dome closure. *Self-assembly of multi-wall tubes* is favored by a stabilizing "lip-lip" interaction between the open edges of adjacent walls. The strong covalent "lip-lip" bonds, mediated by carbon atoms, both passivate the tubes at the growing edge and help to inhibit premature dome closure.

In high applied electric fields, chiral nanotubes disintegrate by *unraveling an atomic wire of carbon* from the edge. The driving force for this process is mainly the gain in polarization energy. The monatomic carbon "wire" is the "ultimate field emitter", capable of sustaining currents of up to $I = 1 \mu\text{A}$.

Acknowledgment

This work has been performed in collaboration with (alphabetically) Richard Enbody, Philippe Jund, Seong Gon Kim, Young Kyun Kwon, Young Hee Lee, Richard E. Smalley, and Weiqing Zhong. The author's participation at the IWFA'97 symposium was partly supported by the organizing committee and a travel grant from Michigan State University. In its early stage, this research was supported by the National Science Foundation under Grant Number PHY-92-24745 and the Office of Naval Research under Grant Number N00014-90-J-1396.

References

1. H.W. Kroto, J.R. Heath, S.C. O'Brien., R.F. Curl, and R.E. Smalley. *Nature*, **318**, 162 (1985).
2. M. S. Dresselhaus, G Dresselhaus, and P.C. Eklund. *Science of Fullerenes and Carbon Nanotubes*, Academic Press Inc., San Diego, 1996 and references therein.
3. S. Iijima. *Nature*, **354**, 56 (1991).
4. T.W. Ebbesen, *Physics Today*, **49** (6), 26 (1996).
5. S. Iijima and T. Ichihashi. *Nature*, **363**, 603 (1993).
6. D. S. Bethune, C. H. Kiang, M. S. deVries, G. Gorman, R. Savoy, J. Vazquez, and R. Beyers. *Nature (London)*, **363**, 605 (1993).

7. M. Tomita, Y. Saito, and T. Hayashi. *Jpn. J. Appl. Phys.*, **32**, L280 (1993).
8. P. M. Ajayan, J. M. Lambert, P. Bernier, L. Barbedette, C. Colliex, and J. M. Planeix. *Chem. Phys. Lett.*, **215**, 509 (1993).
9. J. M. Lambert, P. M. Ajayan, P. Bernier, J. M. Planeix, V. Brotons, B. Coq, and J. Castaing. *Chem. Phys. Lett.*, **226**, 364 (1994).
10. A. Thess, R. Lee, P. Nikolaev, H. Dai, P. Petit, J. Robert, C. Xu, Y.H. Lee, S.G. Kim, D.T. Colbert, G. Scuseria, D. Tománek, J. E. Fisher, and R. E. Smalley. *Science*, **273**, 483 (1996).
11. T. Guo, P. Nikolaev, A.G. Rinzler, D. Tománek, D.T. Colbert, and R.E. Smalley. *J. Phys. Chem.*, **99**, 10694 (1995).
12. T. Guo, P. Nikolaev, A. Thess, D. T. Colbert, and R. E. Smalley. *Chem. Phys. Lett.*, **243**, 49 (1995).
13. S. Witanachchi, and P. Mukherjee. *J. Vac. Sci. Technol.*, **13A**, 1171 (1995).
14. R.E. Smalley. *Mater. Sci. Eng.*, **19B**, 1 (1993).
15. Y. Saito, T. Yoshikawa, M. Inagaki, M. Tomita, and T. Hayashi. *Chem. Phys. Lett.*, **204**, 277 (1993).
16. T.W. Ebbesen. *Annu. Rev. Mater. Sci.*, **24**, 235 (1994).
17. A. Maiti, C.J. Brabec, C.M. Roland, and J. Bernholc. *Phys. Rev. Lett.*, **73**, 2468 (1994).
18. M. Ge, and K. Sattler. *Appl. Phys. Lett.*, **65**, 2284 (1994); *Chem. Phys. Lett.*, **220**, 192 (1994); *Appl. Phys. Lett.*, **64**, 710 (1994); *Science*, **260**, 515 (1993).
19. L.A. Chernozatonskij, Z.Ja. Kosakovskaja, A.N. Kiselev, and N.A. Kiselev. *Chem. Phys. Lett.*, **228**, 94 (1994).
20. W.G. Hoover. *Phys. Rev. A*, **31**, 1695 (1985); S. Nose. *Mol. Phys.*, **52**, 255 (1984).
21. P. Hohenberg, and W. Kohn. *Phys. Rev.*, **136**, B864 (1964); W. Kohn, and L.J. Sham. *Phys. Rev.*, **140**, (1965).
22. U. Von Barth, and L. Hedin. *J. Phys. C*, **5**, 1629 (1972).
23. A. D. Becke. *J. Chem. Phys.*, **88**, 2547 (1988).
24. D. Tománek, and M.A. Schluter., *Phys. Rev. Lett.*, **67**, 2331 (1991).
25. W. Zhong, D. Tománek, and G.F. Bertsch. *Solid State Commun.*, **86**, 607 (1993).
26. R. Saito, M. Fujita, G. Dresselhaus, and M.S. Dresselhaus. *Appl. Phys. Lett.*, **60**, 2204 (1992).
27. N. Hamada, S. Sawada, and A. Oshiyama. *Phys. Rev. Lett.*, **68**, 1579 (1992).
28. Y.H. Lee, S.G. Kim, and D. Tománek. *Phys. Rev. Lett.*, **78**, 2393 (1997).
29. D. Tománek in "Large Clusters of Atoms and Molecules", edited by T.P. Martin, Nato ASI series, **313**, 405 (Kluwer Academic Publishers, Netherlands) (1996).
30. Y.-K. Kwon, Y.H. Lee, S-G. Kim, P. Jund, D. Tománek, and R.E. Smalley. (in preparation).
31. S. Iijima, T. Ichihashi, and Y. Ando. *Nature*, **356**, 776 (1992).
32. G. Overney, W. Zhong, and D. Tománek. *Z. Phys. D.*, **27**, 93 (1993).
33. M.M.J. Treacy, T.W. Ebbesen, and J.M. Gibson. *Nature*, **381**, 678 (1996).
34. A.G. Rinzler, J.H. Hafner, P. Nikolaev, L. Lou, S.G. Kim, D. Tománek, P. Nordlander, D.T. Colbert, and R.E. Smalley. *Science*, **269**, 1550 (1995).
35. W.A. de Heer et al. *Science*, **268**, 845 (1995).
36. W.A. de Heer, A. Châtelain, D. Ugarte. *Science*, **270**, 1179 (1995).
37. Y.H. Lee, S.G. Kim, and D. Tománek. *Chem. Phys. Lett.*, **265**, 667 (1997).
38. V.T. Binh, S.T. Purcell, N. Garcia, J. Doglioni. *Phys. Rev. Lett.*, **69**, 2527 (1992).
39. S. Horch, and R. Morin. *J. Appl. Phys.*, **74**, 3652 (1993).
40. S.G. Kim, Y.H. Lee, P. Nordlander, and D. Tománek. *Chem. Phys. Lett.*, **264**, 345 (1997).